第58卷 第3期
2020年7月

古 脊 椎 动 物 学 报
VERTEBRATA PALASIATICA

pp. 204–220
figs. 1–4

DOI: 10.19615/j.cnki.1000-3118.200514

New *Hystrix* (Hystricidae, Rodentia) from the Neogene of Linxia Basin, Gansu, China

WANG Ban-Yue QIU Zhan-Xiang

(*Institute of Vertebrate Paleontology and Paleoanthropology*, *Chinese Academy of Sciences* Beijing 100044
wangbanyue@ivpp.ac.cn)

Abstract Four well preserved skulls of *Hystrix* recently collected from Linxia Basin were studied and a new species, *H. brevirostra* sp. nov, was established for them. The new species is characterized by its larger size, relatively low and wide skull with short rostrum and diastema, slightly posteriorly convex posterior border of relatively short nasal roughly aligning with lacrimal, shorter and deeply curved mandibular diastema, and relatively low-crowned cheek teeth. It is intermediate between *H. lufengensis* and *H. gansuensis* in evolutionary level, existing in Late Miocene–Pliocene. While it might represent a lineage separated from the above two species. Ontogenetic variation in skull morphology and direction of cheek tooth rows of the new species was also discussed.

Key words Linxia Basin, Gansu; Late Miocene, Liushu Formation; Early Pliocene, Hewangjia Formation; Hystricidae

Citation Wang B Y, Qiu Z X, 2020. New *Hystrix* (Hystricidae, Rodentia) from the Neogene of Linxia Basin, Gansu, China. Vertebrata PalAsiatica, 58(3): 204–220

Hystrix is one of the Old World largest rodents ranging from Late Miocene to recent. Until recently *Hystrix* fossils have been recorded mostly from European Neogene–Quaternay and Asian Quaternary, with only a few from Neogene of Asia (Lydekker, 1884; Wang, 1981; Shevyreva, 1986; Pei, 1987; Sen, 1996, 1999, 2001a, b; Weers and Zhang, 1999). In the last decades records of Neogene *Hystrix* from China have been slowly accumulated (Qiu et al., 1985; Wang and Qiu, 2002; Weers, 2004; Wang and Qi, 2005). Just recently, some new and well preserved *Hystrix* fossils, including 4 skulls, two of them with their mandibles, were collected from Neogene deposits in Linxia Basin. This is the best Neogene material of *Hystrix* so far known from Eurasia. Detailed study of these fossils shows that they not only represent a new species, but also enhance our understanding of *Hystrix* as a whole.

For terminology and method of measurements of the skull and mandible we follow Wang and Qiu (2018), and those of the cheek teeth follow Wang and Qiu (2002).

中国科学院前沿科学重点研究项目(编号：QYZDY-SSW-DQC022)、中国科学院战略性先导科技专项(B类)(编号：XDB26000000) 和国家自然科学基金重点项目(批准号：41430102)资助。

收稿日期：2020-03-20

1 Systematic paleontology

Hystricidae Fischer de Waldheim, 1817

***Hysrix* Linnaeus, 1758**

***Hystrix brevirostra* sp. nov.**

(Figs. 1–4; Tables 1–2)

Hystrix gansuensis: Deng et al., 2011, p. 455, fig. 4a; Deng et al., 2013, p. 260

Holotype A nearly complete skull (but the basioccipital is slightly displaced from its original position) with mandible and a thoracic vertebra [HMV (Catalogue number of the Hezheng Paleozoological Museum of Gansu) 2002], from locality LX 200701 (= Loc. 60 of Zhao Rong), Duikang, Zhuangkeji Village, Guanghe County; Early Pliocene Hewangjia Formation.

Paratype Partial skull (lacking occipital part) with mandible (HMV 2003), from the same locality and horizon as the holotype.

Referred specimens A nearly complete skull (IVPP V 26033) from LX 200205 (= Loc. 54 of Zhao Rong), Baihuacun, Zhuangkeji Village, Guanghe County, upper part of the Liushu Formation, Late Miocene; and a complete skull (HMV 2004=X 2587), from LX 200041, Laohuwo of Shanchengcun, Maijiaji Village, Hezheng County, upper part of Liushu Formation, Late Miocene.

Diagnosis Large-sized *Hystrix*. Skull low and wide, with relatively short rostrum and diastema; nasal relatively short, with posteriorly convex posterior border nearly aligned with the lacrimal. Horizontal ramus of mandible low, with a shorter and deeply concave diastema. Cheek teeth unilaterally subhypsodont, relatively low-crowned; sinus separated from both fold I and fold II in Dp4 and extending into mesoloph in P4.

Etymology brevirostra: brevi, Latin, short; rostra, Latin, feminine, nose. It means that the animal has a relatively short rostrum.

2 Description

2.1 Skull

According to the age-classes of the skulls proposed by Weers (1990), the skulls of HMV 2002, HMV 2003 and IVPP V 26033 are young and belong to age-class IV, while HMV 2004 is adult and belongs to age-class VI.

The skulls are of the hystricomorphous type, relatively low and wide, and have a large infraorbital foramen (Figs. 1–3).

Dorsal view The skull is long ovoid in outline, with relatively narrow rostrum and occipital part. The nasals (N) are slightly longer than wide, with a slightly convex dorsal surface and a posteriorly convex posterior border, which is located much more posteriorly than the premaxillo-frontal suture and nearly aligned with the lacrimal. The premaxillo-frontal suture extends transversely. The maxillo-frontal suture extends obliquely, from the premaxillo-

frontal suture to the lacrimal. The lacrimal (L) is situated mainly within the orbit, with only a small part exposed on the dorsal side at the anteromesial corner of the orbit, where a distinct lacrimal tubercle (lt) forms. The orbit is large and the postorbital process (pp) is distinct. The frontals (F) are wide and have convex dorsal surface, but shorter than the nasals. The fronto-parietal suture is M–shaped, roughly aligns with the posterior zygomatic root. Starting from the postorbital processes, the two weak parietal crests (pc) are convergent posteriorly to meet each other forming a short sagittal crest (sc), which reaches to the distinct nuchal crest (nc).

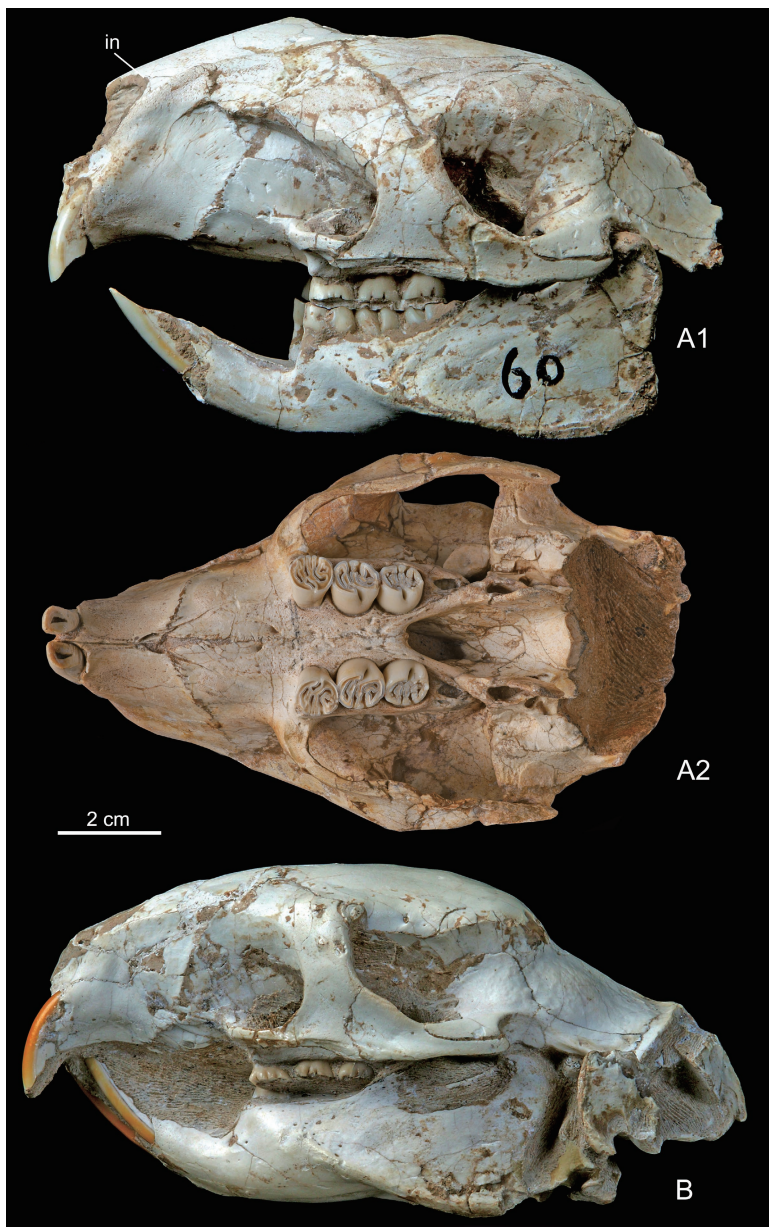

Fig. 1 Skulls and mandibles of *Hystrix brevirostra* sp. nov. from Linxia Basin, Gansu
A. HMV 2003 (paratype): A1. left view of skull with mandible, A2. occlusal view of skull;
B. HMV 2002 (holotype): left view of skull with mandible. Abbreviation: in. *incisura nasomaxilla*

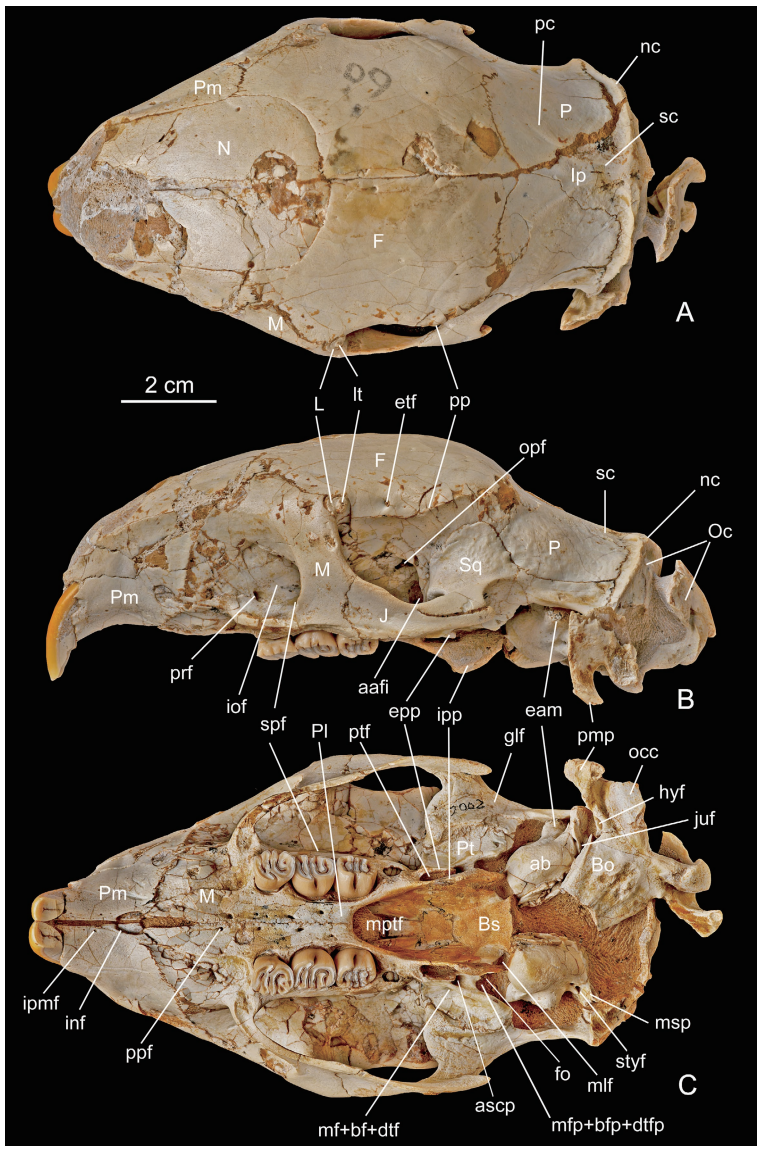

Fig. 2 Skull of *Hystrix brevirostra* sp. nov. (HMV 2002, holotype) from Linxia Basin, Gansu
A. dorsal view; B. left view; C. occlusal view

Abbreviations of bones: Bo. basioccipital; Bs. basisphenoid; F. frontal; Ip. interparietal; J. Jugal; L. lacrimal; M. maxilla; N. nasal; Oc. occipital; P. parietal; Pl. palatine; Pm. premaxilla; Pt. pterygoid; Sq. squamosal
Abbreviations of foramina and other structures: aafi. anterior alar fissure; ab. auditory bulla; ascp. posterior foramen of alisphenoid canal; bf. buccinator foramen; bfp. posterior foramen of buccinator nerve canal; dtf. deep temporal foramen; dtfp. posterior foramen of deep temporal nerve canal; eam. external auditory meatus; epp. external pterygoid process; etf. ethmoidal foramen; fo. *foramen ovale*; glf. glenoid fossa; hyf. hypoglossal foramen; inf. incisive foramen; iof. infraorbital foramen; ipmf. interpremaxilla foramen; ipp. internal pterygoid process; juf. jugular foramen; lt. lacrimal tubercle; mf. masticatory foramen; mfp. posterior foramen of the masseteric nerve canal; mlf. middle lacerate foramen; mptf. mesopterygoid fossa; msp. mastoid process; nc. nuchal crest; occ. occipital condyle; opf. optic foramen; pc. parietal crest; pmp. paramastoid process; pp. postorbital process; ppf. posterior palatine foramen; prf. premolar foramen; ptf. pterygoid fossa; sc. sagittal crest; spf. sphenopalatine foramen; styf. stylomastoid foramen

The parietal (P) is slightly smaller than the frontal and has slightly concave surface. The interparietal (Ip) is bell-shaped, inserting between the two parietals.

Lateral view The skull is relatively low, with a slightly convex roof. The anterior end of the nasal is situated posterior to that of the premaxilla. The *incisura nasomaxilla* (in) is small and shallow. The rostrum is high and short. On the lateral side of the rostrum there is a large concave surface, which is for the insertion of m. *masseter profundus*. The large infraorbital foramen (iof) is within the maxilla and its posterior border is above the M1 in position. The anterior border of the large orbit is situated above M2, and the postorbital process (pp) is above M3 or slightly posterior to M3. The lacrimal tubercle (lt) is located at the anterosuperior corner of the orbit. The bridge between the infraorbital foramen and the orbit is wide and thin-plate in form. The zygomatic arch is formed by zygomatic process of maxilla, jugal (J), and zygomatic process of the squamosal (Sq). The anterior zygomatic root formed from the maxilla is located near the anterior part of DP4 (P4). The anterior part of zygomatic arch (= the inferior margin of infraorbital foramen) is a slim triangular plate, and its posterior part (= inferior margin of orbit) forms a transversely thin and vertically wide plate. The small premolar foramen (prf) is located on the mesial wall of the infraorbital foramen, above the anterior border of Dp4 (P4). The sphenopalatine foramen (spf) is large and located above M1–2. The optic foramen (opf) is relatively small and located above the posterior border of M3 or slightly posterior to M3 and superoposteriorly to the sphenopalatine foramen. The large anterior alar fissure (aafi) is located inferolaterally to the optic foramen. The tiny ethmoidal foramen (etf) is located near the superior border of the orbit and posteriorly to the lacrimal tubercle (lt).

Ventral view The diastema between I2 and DP4 (P4) is short compared with the upper cheek tooth row (ratios of length of diastema to that of P4–M3 are 1.16 and 1.18 in HMV 2004). The incisive foramen (inf) is small and located at the anterior 1/3 of the diastema. A pair of tiny interpremaxillal foramina (ipmf) are located between I2 and inf. The premaxillo-maxillal suture extends anteromesially and passes the posterior end of incisive foramen. On the anterior part of the maxilla there is a pair of bulges showing the positions of the posterior ends of the alveoli of the two I2s. Between the P4 (dp4) and the premaxillo-maxillal suture there is a large concave area, which may be the site for the insertion of m. *buccinator*. In front of P4 (dP4) and near the mid-maxillal suture there is a pair of small posterior palatine foramina (ppf). The left and right cheek tooth rows are slightly convergent posteriorly (in young) or parallel to each other (in adult). On the hard palate between the two teeth rows there are several nutrient foramina. The transversely extending mesial part of the maxillo-palatine suture aligns with the boundary between M1 and M2 (in HMV 2002 and HMV 2003) or with anterior part of M2 (in HMV 2004 and V 26033). The posterior border of the hard palate (= anterior border of the mesopterygoid fossa) is situated mesial to the M2 (in HMV 2002, HMV 2003 and V 26033), or to the anterior part of M3 in adult (HMV 2004), and usually has a small protrusion at the middle. The mesopterygoid fossa (mptf) is large and wide. The pterygoid fossa (ptf) is very narrow and small, with an internal pterygoid process (ipp) higher than the external pterygoid

process (epp). The posterior foramen of alisphenoid canal (ascp) penetrates the posterior part of the external pterygoid process. The masticatory foramen (mf), buccinator foramen (bf) and deep temporal foramen (dtf) are confluent into one foramen. The posterior foramina (mfp, bfp and dtfp) of the three nerve canals mentioned above are also confluent into one, which is located dorsoposterior to the ascp and anteroventral to the *foramen ovale*. The *foramen ovale* (fo) is confluent with the middle lacerate foramen (mlf).

The two zygomatic arches are slightly divergent posteriorly. The glenoid fossa (glf)

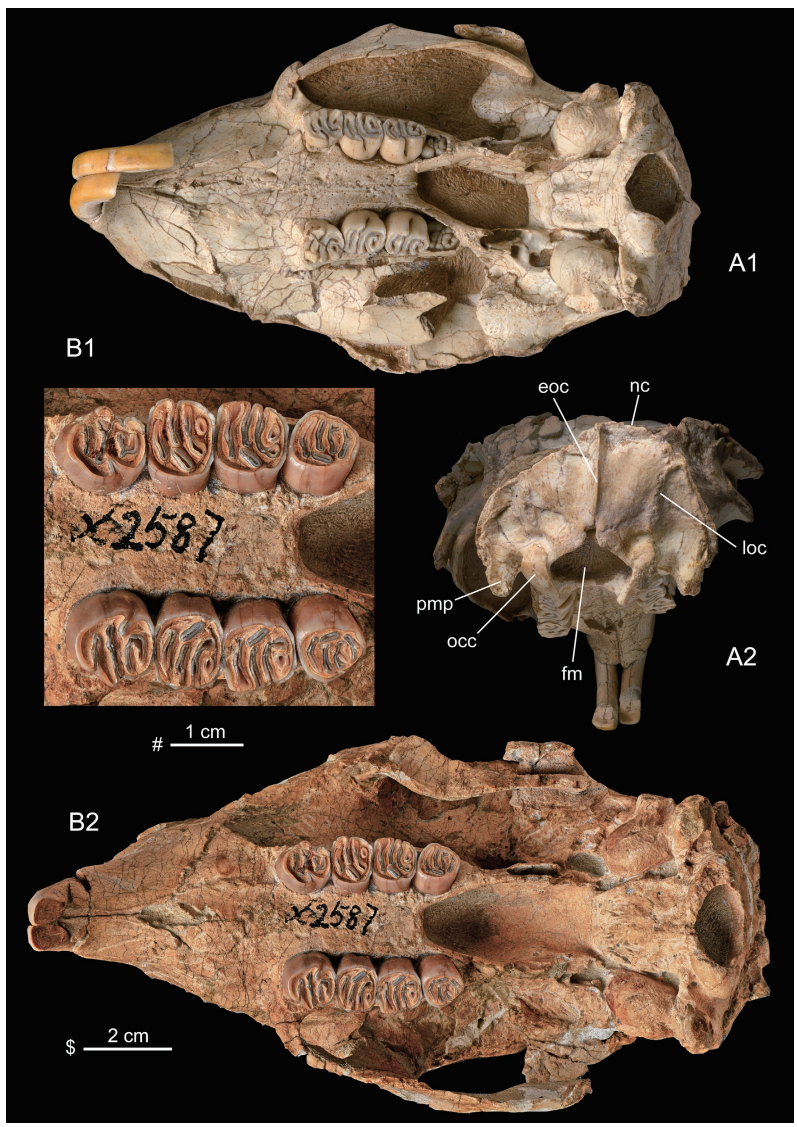

Fig. 3 Skulls of *Hystrix brevirostra* sp. nov. from Linxia Basin, Gansu
A. IVPP V 26033: A1. ventral view, A2. posterior view;
B. HMV 2004: B1. occlusal view of left and right upper cheek teeth, B2. ventral view of skull
Abbreviations: eoc. external occipital crest; fm. *foramen magnum*; loc. lateral occipital crest; nc. nuchal crest; occ. occipital condyle; pmp. paramastoid process. Scales: $ – A1, A2, B2; # – B1

of the squamosal takes a form of short and wide groove which is longitudinally straight but transversely concave. The small auditory bulla (ab) has a short external auditory meatus (eam). The bulla has a spherical surface. The stylomastoid foramen (styf) is located between the bulla and the mastoid process (msp). The jugular foramen (juf) is located mesioposterior to the bulla. The hypoglossal foramen (hyf) is located lateral to the basioccipital and anterior to the occipital condyle (occ).

Posterior view The nuchal surface is about semicircular in outline, rather flat and nearly vertical to the ventral surface of the skull. The external occipital crest (eoc) is developed and extending from nuchal crest (nc) to the superior border of *foramen magnum* (fm). On the two lateral areas of eoc there is a pair of vertical crests, which may be the lateral borders of the area

Table 1 Measurements of skulls and mandibles of *Hystrix brevirostra* sp. nov. from Linxia Basin (mm)

Parameter*	HMV 2002 (holotype) Left/Right	HMV 2003 (paratype) Left/Right	V 26033 (referred specimens) Left/Right	HMV 2004 (referred specimens) Left/Right
1. Condylobasal length (CBL)			138.4	
2. Length of anterior part of skull (LAS)		50		
3. Length of posterior part of skull (LPS)			83.7	104.4
4. Palatal length (PL)		71.2	81.4	
5. Length of maxillary diastema (LMXD)	40.2	42.7	46.5	49
6. Length of palatal bridge (LPB)	45	48.2	55.5	59e
7. Anterior width of palatal bridge (AWPB)	13	11.3	15.3	13
8. Posterior width of palatal bridge (PWPB)	9	8.7	10	13
9. Length of incisive foramen (LIF)	5.5	4	4.4	
10. Rostrum length (RL)		42.6	48e	
11. Anterior width of rostrum (at anterior end of inf) (AWR)	35.5	30	36.2e	37
12. Anterior height of rostrum (at anterior end of inf) (AHR)		35		
13. Posterior width of rostrum (PWR)	53	49		
14. Posterior height of rostrum (PHR)	38.8	47.8		
15. Height of middle part of skull (at anterior border of orbit) (HMS)	39.5	44.3		
16. Nasal length (NL)		67+		
17. Anterior width of nasals (AWN)	29.5e	29e		
18. Posterior width of nasals (PWN)	37	36.6		40.4
19. Interorbital width (IOW)	60.9	62		71.2e
20. Zygomatic width (ZW)	72.5	73e	40×2**	86.4e
21. Width of cranial part at mastoid processes (WCM)			54	
22. Length of auditory bulla (LAB)	17/17.5		18.7/18	17.3
23. Width of auditory bulla (WAB)	11.3/12		12.2/12.5	13.8
24. Distance between two auditory bullae (DAB)			19.5	21.8
25. Nuchal height (NH)			41.1	43
26. Height of foramen magnum (HFM)			13	13.5
27. Width of foramen magnum (WFM)			18	19.5
28. Mandibular length (MDL)	88.5/87.3	93.6		
29. Height of condyloid process of mandible (HCPM)	31.5/30.3	36.3		
30. Length of mandibular diastema (LMD)	24.3/25	25/22		
31. Height of mandiblar diastema (HMD)	13.2/13	13.5/14.4		
32. Height of horizontal ramus of mandible (HHR)	19.5/18.7	20/19		
(12/11) (%)		117		
(14/13) (%)	73.2	97.6		
(15/20) (%)	54.5	61		

* Parameters mainly follow Wang and Qiu (2018) and some are amended here. ** Width of left half part × 2.

for insertion of m. *rectus capitis dorsalis minor*, called here as lateral occipital crests (loc). The paramastoid process (pmp) is developed. The *foramen magnum* is ovoid in outline. The two occipital condyles (occ) are separated widely.

2.2 **Mandible** (Fig. 4)

Both HMV 2002 and HMV 2003 preserve left and right hemimandibles. The mandible is of hystricognathous type, with the angular process extending laterally to the horizontal ramus. The horizontal ramus is straight and low. The symphysis extends posteriorly to below the

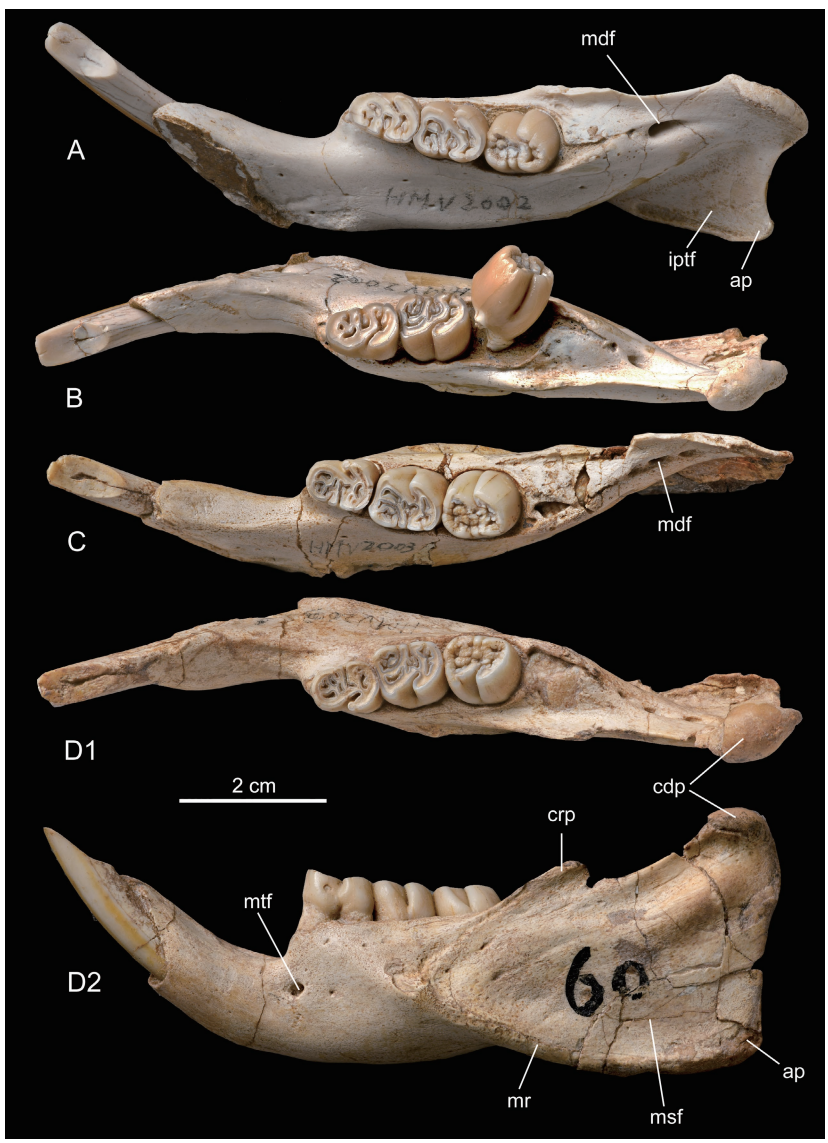

Fig. 4 Mandibles of *Hystrix brevirostra* sp. nov. from Linxia Basin, Gansu
A–B. right (A) and left (B) mandibles of HMV 2002 (holotype) in occlusal views;
C–D. right (C) and left (D) mandibles of HMV 2003 (paratype): C, D1. occlusal view, D2. buccal view
Abbreviations: ap. angular process; cdp. condyloid process; crp. coronoid process; iptf. internal pterygoid fovea; mdf. mandibular foramen; mr. masseteric ridge; msf. masseteric fossa; mtf. mental foramen

anterior root of dp4. The mandibular diastema is shorter than dp4–m2 in length and is deeply concave with a steep posterior part. The mental foramen (mtf) is located below the anterior root of dp4 (p4) in the middle height of buccal side of the horizontal ramus. The masseteric fossa (msf) is large. The distinct masseteric ridge (mr) extends anteriorly to below the m1, nearly at the same horizontal level of the mental foramen. The ascending ramus of mandible is short and low, and extends slightly laterally to the cheek tooth row. The coronoid process (crp) is very low and small, with its anterior border rising from lateral side of horizontal ramus below m1 and its top being slightly higher than the occlusal surface of the lower cheek tooth row. The condyloid process (cdp) is higher and larger than the coronoid process, and has an ovoid-hemispherical articular facet. The angular process (ap) is small and bends slightly lingually below the condyloid process. On the lingual side of the ascending ramus the mandibular foramen (mdf) is situated posterior to the m3. The mdf may be represented by a large single foramen (in HMV 2002) or may be separated into three small ones (in HMV 2003). The internal pterygoid fovea (iptf) is large and deeply concave, with its anterior end extending to below m2 and its lower margin rolling up lingually.

2.3 Teeth

The dental formula is 1·0·1·3/1·0·1·3. The cheek teeth are unilaterally subhypsodont, with the lingual side higher (lower) than the buccal side on the upper (lower) cheek teeth respectively.

The I2 is orthodont, with its anterior end bending ventrally or slightly backwards. In V 26033 the two I2s have longer and more curved anterior parts, which may represent an abnormal phenomenon. The cross section of the I2 is ovoid, with a wider and slightly convex labial surface. The enamel covers the labial side, about 1/3 medial and 1/2 lateral sides. The surface of labial side is smooth and no longitudinal ridge can be seen on it.

P4 and dP4: HMV 2004 is an adult individual and preserves P4–M3. The P4 is the largest of the upper cheek teeth. It is ovoid in outline, slightly longer than wide, with a convex anterior border. The buccal end of fold I is shallowly open (on right P4) or closed with wear (on left P4). Fold II on the right P4 is buccally open, extending upwards almost to the base of the crown on the buccal wall. Fold II on the left P4 is Y-shaped, embracing the enlarged mesostyle. Fold III and IV join together to form a U-shaped fold, which is closed buccally. The protocone joins the anteroloph, protoloph and mesoloph. The anteroloph is shorter than the other lophs. The sinus is short transversely and extends into the mesoloph and does not meet the fold II. Its lingual opening extends upwards almost to the upper 3/5 of the crown height on the lingual side.

HMV 2002, HMV 2003 and V 26033 are all young, and have erupted dP4–M2 and M3 still in alveolus. The dP4 is smaller than M1 in size and trapezoid in outline, slightly longer than wide, with buccal side longer than lingual one. In HMV 2002 and V 26033 the fold I–III remain shallowly open buccally, but in HMV 2003 the buccal end of the anteroloph begins to join the paracone to close fold I on buccal side. In all the dP4, mesoloph, fold III and metaloph

are L-shaped. Fold IV forms a small closed basin. The paracone and mesostyle are usually distinct cusps in HMV 2002 and V 26033, and in HMV 2003 the mesostyle forks buccally. The sinus extends anterobuccally, but does not join with fold I or fold II.

M1 is rectangle in outline, slightly longer than wide in young, but wider than long in adult. In HMV 2002 fold I is open bucally and the paracone extends anteriorly. Thus, the buccal opening of fold I is shallower and easily to be worn out. In the other specimens, fold I is closed buccally. The buccal ends of fold II and III are open shallowly or closed with wear. As in dP4 the mesoloph of M1 is L-shaped and its lingual part extends posteriorly to join the posteroloph. The metaconule is variable: it may be a distinct cusp and the metaloph is only a transverse loph (as in HMV 2002); or it may extend posteriorly to meet the posteroloph forming an L-shaped metaloph (in other specimens). Thus, fold IV may join with fold III to form a U-shaped fold (as in HMV 2002) or may be a closed basin (as in other specimens). In any case, the buccal end of fold IV is closed. The sinus extends anterobuccally to join with fold II in the young, but is separated from the latter in adult. Its lingual end is open and extends upwards to about 1/3 of the crown on the lingual side in young, but closed in adult.

M2 is trapezoid in outline, longer than wide, with a slightly narrower posterior side than anterior side in young, but is rectangular in adult. The other features of M2 are similar to M1.

M3 of HMV 2004 is trapezoid in outline, with shorter and convex lingual and posterior sides. Fold I–IV and the sinus are all closed. The sinus extends nearly longitudinally towards the fold I. Fold III and IV are transversely long folds. M3 of V 26033 is ovoid in outline, longer than wide, with a narrower and convex posterior border. It is unworn, with the occlusal feature similar to that of M2 of HMV 2002.

The i2 is slightly curved and its anterior part extends anterosuperiorly, and the posterior end extends posteriorly to the mandibular foramen. The cross section of the i2 is narrowly ovoid, with a slightly convex labial surface. As in the I2, the enamel covers the labial side, 1/3 medial and 1/2 lateral sides. The surface of labial side is smooth and no longitudinal ridge is seen on it.

The dp4 is ovoid in outline, longer than wide and with a narrow and convex anterior border. Fold I is a small closed basin. The metalophid curves anteriorly, with its middle part meeting the mesolophid to separate fold II into two parts: the lingual one may open lingually (in HMV 2002) or may be closed (in HMV 2003); the buccal one is a closed fold. The mesolophid is variable: it may be a single lophid, or may be separated by small folds into several ones. Fold III is open lingually. Fold IV is closed lingually. There are some protrusions in fold III and IV. The sinusid is open buccally and its lingual end may or may not join with fold IV. The dp4 has three roots: a large anterior one and two small posterior ones.

The m1 is rectangular in outline, longer than wide. The metalophid is a very small circle and closes fold I into a very tiny basin. The mesolophid curves anteriorly to meet the anterolophid. Thus, fold II is L-shaped or U-shaped. Its lingual end is open. The hypolophid is long and may or may not join the posterior arm of the protoconid. Fold III is long and curved,

and sometimes there are some small protrusions in it. Fold IV may or may not join with the sinusid, and there are also some protrusions in it. The lingual openings of fold II–IV are very shallow and easily to be closed with wear. The buccal opening of the sinusid is deep and extends downwards nearly to the 2/3 crown height on the buccal side.

Table 2 Measurements of teeth of *Hystrix brevirostra* sp. nov. from Linxia Basin, Gansu (mm)

Parameter*		HMV 2002 (holotype)		HMV 2003 (paratype)		V 26033 (referred specimens)		HMV 2004	
		Left	Right	Left	Right	Left	Right	Left	Right
P4–M3	L							42.2	41.5
M1–3	L							29.4	29.2
P4 (DP4)	L	9	9	8.8	8.6	9.3	9.5	11.5	11.5
	Wc	7.5	7.5	8.2	8.2	8.1	8.3	10.5	11.2
	Wm	7.9	7.7	8.5	8.4			11.1	13
	Hps	4.5	4.5	4.5	4.5	5	5		
	Hpb1	1.2	1.7			2.5			
	Hpb2	1.5	1.8	2.5	2.5	2.4	2.2		
	Hpb3	1.5	1.5	2.4	2.2	2	2		
M1	L	9	9	9.4	9.3	9.5	10	9.5	9.6
	Wc	7.4	7.5	8	7.8	8.2	8.1	11.4	11.5
	Wm	8	8	9.3	9.2	9.1	9.2	12.3	12.5
M2	L	9	9	9	9	10.2	10.3	10.5	10.4
	Wc	7	6.5	7	7	7.2	7.6	11	10.6
	Wm	7.9	8	8.8	8.7	9.1	9.2	11.8	11.8
M3	L							9.6	9.7
	Wc							9	8.8
	Wm							10.4	10.5
I2	T	6.7	7	6.9	6.9	7.2	7	8.2	8.4
	W	5.5	5.5	5.5	5.5	5.9	5.8	6.2	6.4
dp4	L	10	10	9.5	9.5				
	Wc	6.4	6.8	7	6.9				
	Wm	7	7.5	7.2	7.2				
	Hb	6.7	6	6.1	6.2				
	Hpsd	5	5	4.1	4.2				
	Hl	4.5	4.5	5.7	5.5				
	Hpl3	4	3	4	4				
m1	L	9.8	10	10	10				
	Wc	7	7.3	7.8	7.3				
	Wm	8	8.2	8.3	8.5				
m2	L	9.9	10	10	10				
	Wc	7.5	7.2	7.2	7				
	Wm	8.8	8.6	8.9	9.3				
	Hb	10.6							
	Hpsd	4.4							
	Hl	8.2							
	Hpl2	6							
	Hpl3	6							
	(Hb/L) (%)	107							
i2	T	6	5.9	6.1	6.4				
	W	5.4	5.3	5.2	5.3				

* Parameters follow Wang and Qiu (2018).

Abbreviations: Hb. enamel height of buccal side; Hl. enamel height of lingual side; Hpb1–3. hypsodonty proxy of buccal fold I–III; Hpl2–3. hypsodonty proxy of lingual fold II–III; Hps. hypsodonty proxy of sinus; Hpsd. hypsodonty proxy of sinusid; L. length; T. thickness of incisor; W. width; Wc. width of occlusal surface of cheek teeth; Wm. maximum width of cheek teeth.

The m2 is similar to m1 in outline and structure. But it is scarcely worn and no dentine is seen on the occlusal surface. The m2 has four roots: two small anterior and two large posterior ones.

2.4 Vertebra

The thoracic vertebra of HMV 2002 preserves spinous process, vertebral body, pedicle, transverse process, pre- and postzygapophyses. The long spinous process extends vertically, with ridged anterior and posterior borders. The vertebral body is short. The caput and vertebral fossa are triangle-shaped, but their epiphyses are lost. On either of the left and right lateral borders of the caput and vertebral fossa there is an articular facet for the head of the rib. The prezygapophysis extends forwards from the pedicle. The articular facet on the prezygapophysis is oval in outline, slightly concave, facing superomesially. The postzygapophysis is located on the posterior part of the pedicle. The articular facet on the postzygapophysis is oval, slightly concave, and facing inferomesially. The robust transverse process extends laterally from the pedicle, situated lower than the pre- and postzygapophyses in position. Its distal end is damaged.

3 Comparison

The above described skulls are similar to the genus *Hystrix* rather than to *Atherurus* and *Trichys* in being large in size; skull having convex roof, enlarged nasal cavity; long and wide nasal with a convex dorsal surface and posteriorly convex posterior border; frontal being shorter than nasal, but larger than parietal in size; having large infraorbital foramen and small and round auditory bulla, etc.

In comparison with the known Pleistocene and living species of *Hystrix*, including *H. brachyura*, *H. subcristata*, *H. hodgsoni*, *H. cristata*, *H. indica*, *H. javanica*, *H. kiangsenensis*, *H. largrelii*, *H. zhengi* and *H. magna* etc. (Lönnberg, 1924; Wang, 1981; Pei, 1987; Weers, 1990; Huang et al., 1995; Guo, 1997; Weers and Zheng, 1998; Sen 1999; Weers and Zhang, 1999; Tong, 2005; Weers, 2005; Pan et al., 2007), the specimens described above are different from them in cheek teeth being lower crowned. Besides, the specimens are larger than *H. brachyura*, *H. subcristata*, *H. hodgsoni*, *H. cristata*, *H. indica*, *H. javanica*, *H. kiangsenensis* and *H. largrelii* in size. In addition, they differ from *H. lagrelii*, *H. brachyura*, *H. indica* and *H. javanica* in having enlarged nasal; from *H. hodgsoni*, *H. subcristata* and *H. magna*[1)] in skull being lower and wider, with less vaulted dorsal surface, smaller nasal cavity and shorter nasal.

1) *Hystrix magna* was erected by Pei (1987). When he described the new species *H. magna*, Pei (1987) did not mention the holotype of the new species. Later, Weers and Zheng (1998) chose the left M1/2 (IVPP V 5036.12) from the specimens described by Pei (1987) as the lectotype of *H. magna*. However, having not mention the paper of Weers and Zheng (1998), Wang (2019:336) once again chose a lectotype for *H. magna*, the right P4 (IVPP V 11550.2) described by Weers and Zhang (1999). It seems to us that the lectotype of *H. magna* should be the left M1/2 (V 5036.12) rather than the right P4 (V 11550.2).

Neogene *Hystrix* is known including 11 species: *H. parvae*, *H. primigenia*, *H. sivalensis*, *H. leakeyi*, *H. refossa*, *H. depereti*, *H. aryaensis*, *H. trofimovi*, *H. caucasica*, *H. gansuensis* and *H. lufengensis* (Shevyreva, 1986; Weers, 1994; Weers and Montoya, 1996; Sen, 1996, 1999, 2001a, b; Wang and Qiu, 2002; Weers and Rook, 2003; Lopatin et al., 2003; Wang and Qi, 2005; Sen and Purabrishemi, 2010).

In comparison with these Neogene species of *Hystrix* the specimens described above are larger than *H. parvae*, *H. leakeyi* and *H. aryaensis*; the crowns of their cheek teeth are higher than those of *H. parvae*, *H. primigenia*, *H. sivalensis*, *H. trofimovi* and *H. lufengensis*, but lower than those of *H. leakeyi*, *H. refossa*, *H. depereti*, *H. aryaensis*, *H. caucasica* and *H. gansuensis*. In addition, they differ from *H. primigenia*, *H. gansuensis*, *H. depereti* and *H. lufengensis* in having shorter rostrum; from *H. gansuensis* and *H. depereti* in having shorter nasal; from *H. primigenia*, *H. refossa*, *H. depereti* and *H. lufengensis* in having lower horizontal ramus of mandible, and shorter and deeper concave mandibular diastema. Besides, they differ from all of the known species of *Hystrix* in P4 having sinus extending into mesoloph, and from *H. gasuensis* in sinus of dP4 being separated from fold I.

The above comparison tends to show that the new specimens described above represent a new species of *Hystrix*, named as *H. brevirostra* here.

4 Discussion

Deng et al. (2011:455, fig. 4a) referred a skull (without mentioning the catalogue number) from Duikang (LX 200701) to *Hystrix gansuensis*, a species established by Wang and Qiu in 2002. According to their figure 4a, this specimen should be the HMV 2003, the paratype of *H. brevirostra* described in this paper. As noted above, this skull (HMV 2003) is different from *H. gansuensis* in having shorter rostrum and nasal, cheek teeth being lower crowned and differing in occlusal features. The skull (HMV 2003) should be referred to the new species, *H. brevirostra* rather than to *H. gansuensis* as Deng et al. (2011, 2013) did.

There are considerable ontogenetic variations in *Hystrix brevirostra*: among the four skulls three (HMV 2002, 2003 and V 26033) are young and one (HMV 2004) is an adult individual. Although all the three young skulls are lumped to IV stage based on Weers (1990), their individual ages are not the same: in HMV 2002 and HMV 2003 the M3 are still in their alveoli, while in V 26033 M3 begins to erupt. Thus, V 26033 is slightly elder than the other two in age. In observing and describing the skulls we found the following variations in the four skulls:

(1) The posterior border of the hard palatine is variable in position: it alignes with the sinus of M2 in HMV 2002 and HMV 2003, with the posterior part of M2 in V 26033, and with the anterior part of M3 in HMV 2004. It would mean that the posterior border of the hard palatine of *H. brevirostra* moves posteriorly with age in young individuals.

(2) The posterior border of nasal is above M2 (in young), but moves to above M3 (in adult) in the position, again moving posteriorly with age in young individuals.

(3) The two upper tooth rows are slightly convergent posteriorly in young individuals, but parallel to each other in adult.

Wang and Qiu (2002) discussed the evolutionary tendencies among the species of *Hystrix*. Most of these evolutionary tendencies are substantiated by the new species. They are: skull changed from relatively lower and wider to higher and narrower in proportion; the rostrum became higher; the nasals and frontals enlarged; the crown of the cheek teeth became more hypsodont; and M3/m3 became reduced. Based on these evolutionary tendencies, it is obvious that *H. brevirostra* is more primitive than all of the Pleistocene and living species of *Hystrix*.

Up to now only three species of *Hystrix* are known from Neogene of China. They are *H. gansuensis*, *H. lufengensis* and *H. brevirostra*. As stated above, *H. brevirostra* differs from *H. gansuensis* in skull having shorter rostrum and nasal, and cheek teeth being lower crowned. On the contrary, the cheek teeth of *H. brevirostra* are higher crowned than those of *H. lufengensis*. Thus, *H. brevirostra* is slightly more progressive than *H. lufengensis*, but more primitive than *H. gansuensis*. However, *H. breviostra* has a shorter rostrum than the other two species. Therefore, *H. breviostra* may represent a different evolutionary lineage as the other two species.

Compared with other Neogene species of *Hystrix* outside China, based on the crown height of the cheek teeth, it seems that *H. brevirostra* is more advanced than *H. parvae*, *H. primigenia*, *H. sivalensis* and *H. trofimovi*, but more primitive than *H. leakeyi*, *H. refossa*, *H. depereti*, *H. aryaensis* and *H. caucasica*. However, this should be further testified by more convincing material to be discovered in future.

The specimens of *H. brevirostra* are collected from three different localities: HMV 2002 and HMV 2003 from Duikang (LX 200701), IVPP V 26033 from Baihuacun (LX 200205), and HMV 2004 from Shanchengcun (LX 200041). The geologic age of Duikang is known to be Lower Pliocene (Hewangjia Formation, Deng et al., 2011). The other fossils from Baihuacun (LX 200205) are known to include four species: *Gazella* cf. *G. gaudryi*, *G. paotehensis*, *Hipparion coelophyes* and *H. hippidiodus* (Deng et al., 2013; Li, 2014). Among them the first three are known from Late Miocene Yangjiashan fauna. The last one, *H. hippidiodus*, has been known from Late Miocene deposits of Qingyang. The fauna from Baihuacun may be correlated with the Late Miocene Yangjiashan fauna.

The other fossils from Shanchengcun (LX 200041) are known to include 6 species: *Hipparion weihoensis*, *Acerorhinus hezhengensis*, *Chilotherium wimani*, *Chleuastrochoerus stehlini*, *Cervavitus novorassiae* and *Muntiacus* sp. According to Deng et al., 2013, *H. weihoensis* has been known to be early–middle Bahean ranging from Guoligou Fauna to Dashengou Fauna in age; *A. hezhengensis*, *Chi. wimani* and *Chl. stehlini* are known to be middle–late Bahean ranging from Dashengou Fauna to Yangjiashan Fauna in age; *C. novorassiae* is known to range from late Bahean Yangjiashan Fauna to Early Pliocene in age. *Muntiacus* is known to range from Late Miocene to Recent. It seems that the fauna from Shanchengcun can also be correlated with the Late Miocene Yangjiashan Fauna.

To sum up, *Hystrix brevirosta* ranges from Late Miocene late Bahean to Early Pliocene Gaozhuangian in age.

Acknowledgments The authors would like to express their gratitude to Director He-Wen and Vice director Cheng Shan-Qin of the Hezheng Paleozoological Museum of Gansu (HPM) for kindly permitting the authors to study the specimens of HPM. The authors are also greatly indebted to the following colleagues of IVPP: to Profs. Zheng Shao-Hua, Ni Xi-Jun and Zhang Zhao-Qun for their valuable discussion; to Profs. Ni Xi-Jun, Deng Tao, Wang Shi-Qi, Wang Yuan and Tong Hao-Wen for their multifarious help, and to Profs. Qiu Zhu-Ding and Zhang Zhao-Qun for their careful review of the manuscript and their valuable suggestions to improve the text of the paper. Many thanks are also given to Mr. Wang Ping for his careful and skillful preparation of the studied fossils, to Mr. Gao Wei for the photographs, and to Mrs. Si Hong-Wei for her help in preparing the pictures.

豪猪化石在临夏盆地的新发现

王伴月　　邱占祥

(中国科学院古脊椎动物与古人类研究所 北京 100044)

摘要：近年来，在甘肃临夏盆地又发现了4件豪猪类的头骨化石，它们属于*Hystrix*的一新种，被命名为短吻豪猪(*Hystrix brevirostra*)。该种的主要特征是，个体大，头骨相对较低宽，吻部和齿隙较短，较短的鼻骨的后缘为向后凸的弧形，其后端约与泪骨相对。下颌骨的下齿隙较短，凹入较深。颊齿齿冠较*H. gansuensis*者稍低，较*H. lufengensis*者稍高。DP4的舌侧沟不与颊侧褶I相连，P4的舌侧沟伸向中脊，不与颊侧褶II相连。邓涛等(2011)曾将产于对康的一件豪猪头骨化石鉴定为*H. gansuensis*。现研究表明，他们描述的标本(HMV 2003)应属于不同于*H. gansuensis*的新种：*H. brevirostra*。将*H. brevirostra* (新种)的幼年的头骨与成年的头骨比较后发现，豪猪头骨的一些特征随着年龄的增长而有所变化：硬腭和鼻骨后缘的相对位置均随着年龄的增长而逐渐后移，两上颊齿列在幼年彼此稍向后靠近，但在成年则彼此平行等。关于百花村(LX 200205)和山城(LX 200041)两地点产豪猪化石层位的时代，根据共生的哺乳动物群分析，其时代为晚中新世晚期。产于我国新近纪的豪猪化石目前仅已知3种(*H. gansuensis*, *H. lufengensis*和*H. brevirostra*)。新种*H. brevirostra*可能比*H. lufengensis*稍进步，但较*H. gansuensis*稍原始。由于*H. brevirostra*的吻部较*H. gansuensis*和*H. lufengensis*者都短，它可能代表不同于该两种的另一进化支系。

关键词：甘肃临夏盆地，晚中新世柳树组，早上新世何王家组，豪猪科

中图法分类号：Q915.873　　**文献标识码**：A　　**文章编号**：1000–3118(2020)03–0204–17

References

Deng T, Hou S K, Shi Q Q et al., 2011. Terrestrial Mio-Pliocene boundary in the Linxia Basin, Gansu, China. Acta Geol Sin, 85(2): 452–464

Deng T, Qiu Z X, Wang B Y et al., 2013. Late Cenozoic biostratigraphy of the Linxia Basin, northwestern China. In: Wang X M, Flynn L J, Fortelius M eds. Fossil Mammals of Asia: Neogene Biostratigraphy and Chronology. New York: Columbia University Press. 243–273

Guo J W, 1997. Note on a fossil skull of *Hystrix magna* Pei, 1987 (Rodentia, Mammalia) from Chongzuo, Guangxi. Vert PalAsiat, 35(2): 145–153

Huang W J, Chen Y X, Wen Y X, 1995. Rodents of China. Shanghai: Fudan University Press. 1–308

Li Y K, 2014. Study of *Gazella* fossils in the Yangjiashan fauna from the Linxia Basin, Gansu Province. Master's Thesis. Beijing: University of Chinese Academy of Sciences. 1–73

Lönnberg E, 1924. On a new fossil porcupine from Honan with some remarks about the development of the Hystridae. Palaeont Sin, Ser C, 1(3): 1–15

Lopatin A V, Tesakov A S, Titov V V, 2003. Late Miocene–Early Pliocene porcupines (Rodentia, Hystricidae) from south European Russia. Russ J Theriol, 2(1): 26–32

Lydekker R, 1884. Indian Tertiary and post-Tertiary vertebrata. Part 3. Rodents, new ruminants from the Siwaliks and synopsis of Mammalia. Mem Geol Surv India Paleont, Ser 10, 3: 105–134

Pan Q H, Wang Y X, Yan K, 2007. A Field Guide to the Mammals of China. Beijing: China Forestry Publishing House. 1–420

Pei W Z, 1987. Carnivora, Proboscidea and Rodentia from Liucheng *Gigantopithecus* cave and other caves in Guanxi. Mem Inst Vert Palaeont Palaeoanthrop, Acad Sin, 18: 5–134

Qiu Z D, Han D F, Qi G Q et al., 1985. A preliminary report on a micromammalian assemblage from the hominoid locality of Lufeng, Yunnan. Acta Anthrop Sin, 4(1): 13–32

Sen S, 1996. Late Miocene Hystricidae in Europe and Analonia. In: Berno R L, Fahlbusch V, Mittmann W eds. The Evolution of Western Eurasian Neogene Mammal Fauna. New York: Columbia University Press. 264–265

Sen S, 1999. Family Hystricidae. In: Rössner G E, Heissig K eds. The Miocene Land Mammals of Europe. München: Verlag Dr. Friedrich Pfeil. 427–434

Sen S, 2001a. Early Pliocene porcupine (Mammalia, Rodentia) from Perpignan, France: a new systematic study. Geodiversitas, 23(2): 303–312

Sen S, 2001b. Rodents and insectivores from the Upper Miocene of Molayan, Afghanistan. Palaeontology, 44(5): 913–932

Sen S, Purabrishemi Z, 2010. First porcupine fossils (Mammalia, Rodentia) from the Late Miocene of NW Iran, with notes on Late Miocene–Pliocene dispersal of porcupines. Paläont Z, 84: 239–248

Shevyreva N S, 1986. The new porcupine (Hystricidae, Rodentia, Mammalia) from the Pliocene of Tadjikistan. Tr Zool Inst Akad Nauk SSSR, 156: 118–133

Tong H W, 2005. *Hystrix subcristata* (Mammalia, Rodentia) from Tianyuan Cave, a human fossil site newly discovered near Zhoukoudian (Choukoutien). Vert PalAsiat, 43(2): 135–150

Wang B Y, Qi G Q, 2005. A porcupine (Rodentia, Mammalia) from *Lufengpithecus* site, Lufeng, Yunnan. Vert PalAsiat, 43(1): 11–23

Wang B Y, Qiu Z X, 2002. A porcupine from the Late Miocene of Linxia Basin, Gansu, China. Vert PalAsiat, 40(1): 23–33

Wang B Y, Qiu Z X, 2018. Late Miocene pararhizomyines from Linxia Basin of Gansu, China. Palaeont Sin, New Ser C, 31: 1–271

Wang K M, 1981. Die Hohlenablagerungen und fauna in der Drachen-Maul-Hohle von Kiangsen, Chekiang. Contrib Natl Res Inst Geol, Akad Sin, 1: 41–67

Wang Y, 2019. Family Hystricidae Fish de Waldheim, 1817. In: Li C K, Qiu Z D eds. Palaeovertebrata Sinica, Vol. III Fasc. 5(1). Beijing: Science Press. 327–341

Weers D J van, 1990. Dimensions and occlusal patterns in molars of *Hystrix brachyura* Linnaeus, 1758 (Mammalia, Rodentia) in a system of wear categories. Bijdr Dierkd, 60(2): 121–134

Weers D J van, 1994. The porcupine *Hystrix refossa* Gervais, 1852 from the Plio–Pleistocene of Europe, with notes on other fossil and extant species of the genus *Hystrix*. Scripta Geol, 106: 35–52

Weers D J van, 2004. Comparison of Neogene low-crowned *Hystrix* species (Mammalia, Porcupines, Rodentia) from Europe, West and Southeast Asia. Beaufortia, 54(5): 75–80

Weers D J van, 2005. A taxonomic revision of the Pleistocene *Hystrix* (Hystricidae, Rodentia) from Eurasia with notes on the evolution of the family. Contrib Zool, 74(3/4): 301–312

Weers D J van, Montoya P, 1996. Taxonomy and stratigraphic record of the oldest European porcupine *Hystrix parvae* (Kretzoi, 1951). Proc K Ned Akad Wet, 99(1-2): 131–141

Weers D J van, Rook L, 2003. Turolian and Ruscinian porcupines (genus *Hystrix*, Rodenta) from Europe, Asia and North Africa. Paläont Z, 77(1): 95–113

Weers D J van, Zhang Z Q, 1999. *Hystrix zhengi* n. sp., a brachyodont porcupine (Rodentia) from early Nihewanian stage, Early Pleistocene of China. Beaufortia, 49(7): 55–62

Weers D J van, Zheng S H, 1998. Biometric analysis and taxonomic allocation of Pleistocene *Hystrix* specimens (Rodentia, Porcupines) from China. Beaufortia, 48(4): 47–70